


## ORIGINAL

## ARTICLE



## No evidence for cell-to-cell transmission of the unfolded protein response in cell culture

Anna M. van Ziel\*†, Kimberly Wolzak†, Anna Nölle‡, Petrus J. Hoetjes†, Ernesto Berenjano-Correa\*†, Eelco van Anken§, Eduard A. Struys¶ and Wiep Scheper\*†\*\* 

\*Department of Clinical Genetics, Amsterdam University Medical Centers Location VUmc, Amsterdam, The Netherlands

†Department of Functional Genomics, Center for Neurogenomics and Cognitive Research, Vrije Universiteit (VU), Amsterdam, The Netherlands

‡Department of Pathology, Amsterdam University Medical Centers Location VUmc, Amsterdam, The Netherlands

§Division of Genetics and Cell Biology, San Raffaele Scientific Institute, Milan, Italy

¶Department of Clinical Chemistry, Amsterdam University Medical Centers Location VUmc, Amsterdam, The Netherlands

\*\*Alzheimer Center, Amsterdam University Medical Centers Location VUmc, Amsterdam, The Netherlands

**Abstract**

The unfolded protein response (UPR) is one of the major cell-autonomous proteostatic stress responses. The UPR has been implicated in the pathogenesis of neurodegenerative diseases and is therefore actively investigated as therapeutic target. In this respect, cell non-autonomous effects of the UPR including the reported cell-to-cell transmission of UPR activity may be highly important. A pharmacology-based UPR induction was employed to generate conditioned media (CM) from CM-donating neuronal ('donor') cells (SK-N-SH and primary mouse neurons). As previously reported, upon subsequent transfer of CM to naive neuronal 'acceptor' cells, we confirmed UPR target mRNA and protein expression by qPCR and automated microscopy. However, UPR target gene expression was also induced in the absence of donor cells, indicating carry-over of pharmacology. Genetic induction of single pathways of the UPR in donor cells did not result in UPR transmission to

acceptor cells. Moreover, no transmission was detected upon full UPR activation by nutrient deprivation or inducible expression of the heavy chain of immunoglobulin M in donor HeLa cells. In addition, in direct co-culture of donor cells expressing the immunoglobulin M heavy chain and fluorescent UPR reporter acceptor HeLa cells, UPR transmission was not observed. In conclusion, carry-over of pharmacology is a major confounding factor in pharmacology-based UPR transmission protocols that are therefore unsuitable to study cell-to-cell UPR transmission. In addition, the absence of UPR transmission in non-pharmacology-based models of UPR activation indicates that cell-to-cell UPR transmission does not occur in cell culture.

**Keywords:** cell non-autonomous, endoplasmic reticulum stress, neurodegenerative diseases, proteostasis, unfolded protein response, UPR transmission.

*J. Neurochem.* (2020) **152**, 208–220.

Received May 3, 2019; revised manuscript received July 31, 2019; accepted August 12, 2019.

Address correspondence and reprint requests to Wiep Scheper, VU Faculty of Science, Center for Neurogenomics and Cognitive Research, Department of Functional Genomics, De Boelelaan 1085, 1081 HV Amsterdam, The Netherlands. E-mail: w.scheper@amsterdamumc.nl

**Abbreviations used:** ATF4, activating transcription factor 4; ATF6, activating transcription factor 6; BiP, binding immunoglobulin protein; CHO, Chinese hamster ovary; CHOP, C/EBP homologous protein; CM, conditioned media; DAPI, 4',6-diamidino-2-phenylindole; DMEM,

Dulbecco's Modified Eagle Medium; EEF1A1, eukaryotic translation elongation factor 1 alpha 1; ER, endoplasmic reticulum; FA, formaldehyde; Fv2E-PERK, PERK coupled to 2 Fv receptor domains; GFPd2, destabilized green fluorescent protein; IgM, immunoglobulin M; IRE1, inositol requiring enzyme 1; LPS, lipopolysaccharide; Mif, mifepristone; PERK, protein kinase R (PKR)-like ER kinase; RRID, Research Resource Identifier (see scicrunch.org); TG, thapsigargin; TG-CM, CM prepared using TG; TLR4, Toll-like receptor 4; TM, tunicamycin; TM-CM, CM prepared using TM; UPR, unfolded protein response; XBP1s, spliced variant of X-box binding protein 1.

The unfolded protein response (UPR) senses disturbance of the protein homeostasis (proteostasis) in the endoplasmic reticulum (ER), defined as ER stress (Walter and Ron 2011). The UPR is a much investigated mechanism in neurodegenerative diseases due to the common presence of UPR activation markers in patient brains (reviewed in Scheper and Hoozemans 2015) and its potential for therapeutic intervention (Halliday, Hughes, and Mallucci 2017; Gerakis and Hetz 2018). The UPR comprises three branches mediated by stress sensors located in the ER membrane, inositol requiring enzyme 1 (IRE1), protein kinase R (PKR)-like ER kinase (PERK), and activating transcription factor 6 (ATF6). Upon ER stress, downstream signaling cascades are initiated by dissociation of chaperone binding immunoglobulin protein (BiP) from the ER luminal domains of the sensors. The overall aim of the UPR pathways is to restore proteostasis by inducing the transcription of molecular chaperones, transiently decreasing protein synthesis and increasing the clearance of misfolded proteins. If the UPR is unable to restore the proteostatic balance, apoptotic pathways are activated (Walter and Ron 2011).

Regulation of proteostasis was considered to be a cell-autonomous process; however, recently multiple studies reported that proteostasis-related stress signaling can cross cellular and tissue boundaries expanding its range to the entire organism (reviewed in van Oosten-Hawle and Morimoto 2014; Schinzel and Dillin 2015; Zanetti, Rodvold, and Mahadevan 2016). This exchange of information about the proteostatic condition was hypothesized to lead to a more coordinated response by adaptation of recipient cells and tissues, making them more resilient to subsequent proteotoxic stress. Therefore, the concept of ‘danger signaling’ described for the secretion of danger signals upon inflammation (Matzinger 1994), may also apply to proteotoxic stress.

Transmission of full UPR signaling, that is, activation of all three branches of the UPR, has been reported in cell models using transfer of conditioned media (CM) of tumor cells subjected to ER stress, to unstressed macrophages (Mahadevan *et al.* 2011). A similar model in neuronal cells and astrocytes also showed transmission of the signaling by all UPR branches (Sprenkle *et al.*, 2019). In agreement with the danger signaling hypothesis, CM treatment resulted in resistance to subsequent ER stress in these cell-to-cell transmission models (Rodvold *et al.* 2017; Sprenkle *et al.*, 2019).

Neurodegenerative diseases like Alzheimer’s disease and Parkinson’s disease are protein misfolding diseases that are characterized by inclusions of aggregated proteins. Recent evidence indicates that cell-to-cell transmission of aggregating proteins is involved in the spreading of the pathology through the brain and progression of the disease (Goedert

2015). Because the pathology is commonly accompanied by the presence of UPR activation markers (reviewed in Scheper and Hoozemans 2015), transmission of the UPR may potentially contribute to disease pathogenesis. Here we employed the pharmacological cell-to-cell UPR transmission protocol as previously published (Mahadevan *et al.* 2011) as well as different genetic UPR activation tools to study transmission of UPR activation. Our data show no evidence for cell-to-cell transmission of UPR activity in cell culture.

## Materials and methods

### Animals and primary cell culture

Animal experiments are in accordance with institutional and Dutch governmental guidelines and regulations and were approved by the animal ethical committee of the VU University/VU University Medical Center (‘Dier ethische commissie’ license number: FGA 11-03).

For primary neuron cultures, m18-1 wild type (C57BL/6, Research Resource Identifier, RRID:IMSR\_CRL:27 backcrossed for more than 10 times) pregnant female mice aged 4–8 months (Charles River Laboratories Inc., Wilmington, MA, USA and breeding in house) were used. Mice were housed in type 2 cages with 2–3 cage companions and fed *ad libitum*. For isolation of primary neurons, pregnant mice were sacrificed via cervical dislocation and pups were obtained by caesarean section and decapitated at embryonic day 18. Cortical hemispheres of the pups brains were dissected and collected in ice-cold Hanks’ balanced salt solution (Sigma-Aldrich, Zwijndrecht, The Netherlands; H9394-6X1L) with 10 mM HEPES (Gibco, Rockville, MD, USA; 15630080; Hanks-HEPES). 0.25% trypsin (Gibco; 15090046) was added to Hanks-HEPES for digestion and cortices were incubated for 20 min at 37°C. Tissue was washed with Hanks-HEPES and triturated with a 1 mL and a fire-polished Pasteur pipette in Dulbecco’s modified Eagle medium (DMEM; Lonza, Geleen, The Netherlands; LO BE12-604F/U1) supplemented with 10% fetal bovine serum (FBS; Gibco; 26140079) and 1% Pen-Strep (Gibco; 15140122; DMEM<sup>+</sup>). After trituration, cells from multiple brains were pooled and centrifuged (115 g, 5 min) followed by resuspension in neurobasal medium (Gibco; 21103049) supplemented with 2% B27 (Gibco; 17504044), 18 mM HEPES, 0.25% glutamax (Gibco; 35050038) and 0.1% Pen-Strep. Before adding neurons, 6-well plates were coated with a solution of 0.01% poly-L-ornithin (Sigma-Aldrich; P4957) and 2.5 µg/mL laminin (Sigma-Aldrich; L2020). For qPCR, neurons were plated with a density of  $3 \times 10^5$  cells/well and grown at 37°C, 5% CO<sub>2</sub>. Treatments were started after 8–9 days *in vitro*.

### Cell culture and treatments of cell lines

The cell lines used in this study were not listed as commonly misidentified cell lines by the International Cell Line Authentication Committee, no further authentication was performed. Cells were maintained in T75 culture flasks and grown in DMEM<sup>+</sup>, except Chinese hamster ovary (CHO) cells stably expressing PERK coupled to 2 Fv receptor domains (Fv2E-PERK; kind gift from

Dr. D. Ron; Lu *et al.* 2004), these were grown in HAM's F12 medium (Gibco; 11765054) supplemented with 10% fetal bovine serum and 1% Pen-Strep. CHO Fv2E-PERK cells and UPR reporter HeLa cells were cultured in the presence of puromycin (13  $\mu$ M; InvivoGen, Toulouse, France; ant-pr-1) or hygromycin B (350  $\mu$ g/mL; Merck, Darmstadt, Germany; 400050), respectively. Antibiotics were omitted during experiments. SK-N-SH cells (ATCC, LGC Standards GmbH, Wesel, Germany; ATCC<sup>®</sup> HTB-11<sup>™</sup>; RRID:CVCL\_0531) were differentiated into neuronal cells with retinoic acid (10  $\mu$ M; Sigma-Aldrich; R2625) for 5–7 days and THP-1 cells (kind gift from Dr. J. Hoozemans, RRID:CVCL\_0006) were differentiated into a macrophage-like phenotype by addition of phorbol 12-myristate 13-acetate (100 ng/mL; Santa Cruz Biotechnology, Heidelberg, Germany; SC-3576) for 2 days. THP-1 cells were stimulated with lipopolysaccharide (LPS) (100 ng/mL; Sigma-Aldrich; L2630) to activate Toll-like receptor 4 (TLR4).

To initiate nutrient deprivation, SK-N-SH cells were cultured in neurobasal medium without B27 supplement. 2% B27 was added before incubation of the CM on acceptor cells. For qPCR experiments, cells were plated in 12-well plates at the following densities; 1.3–1.5  $\times 10^5$  cells/well SK-N-SH cells, 1  $\times 10^5$  cells/well mifepristone (Mif)-inducible immunoglobulin M (IgM) heavy chain HeLa cells, 4  $\times 10^5$  cells/well THP-1 cells, 1.2  $\times 10^5$  cells/well Fv2E-PERK CHO cells. For immunofluorescence experiments, SK-N-SH and HeLa (ATCC<sup>®</sup> CCL-2<sup>™</sup>; RRID:CVCL\_0030) cells were plated in black 96-well plates (Greiner, Alphen a/d Rijn, The Netherlands; 655090) with a density of 1  $\times 10^4$  cells/well. A density of 3  $\times 10^5$  cells/well was used for western blotting experiments with SK-N-SH and 2.5  $\times 10^5$  cells/well Fv2E-PERK CHO cells in six-well plates. See the co-culture UPR transmission protocol for plating conditions of the UPR reporter assay. Cell lines were maintained at 37°C, 5% CO<sub>2</sub> and not used beyond passage 25.

#### UPR constructs and stable cell lines

PERK signaling in CHO Fv2E-PERK cells was initiated by addition of the B/B Homodimerizer (identical to the AP20187 ligand; Takara Bio, Saint-Germain-en-Laye, France; 635059). The doxycycline (Sigma-Aldrich; D9891)-inducible ATF6 and X-box binding protein 1 (XBP1s) active transcription factor constructs and lentiviral particles and the Mif-inducible IgM heavy chain HeLa cell line were described before (Van Ziel *et al.* 2019 and Bakunts *et al.* 2017, respectively).

HeLa cell lines stably expressing either the activating transcription factor 4 (ATF4) or the ATF6/XBP1s UPR reporter constructs were generated to monitor UPR activation. The 5' untranslated region of human ATF4 fused to the enhanced yellow fluorescent protein plasmid (kind gift from Dr. E. Jan; Lee, Cevallos, and Jan 2009) was C-terminally tagged with a nuclear localization sequence (3  $\times$  PKKKRKV) and cloned into the pcDNA3.1[Hygro] backbone (Invitrogen, Carlsbad, CA, USA; V87020). Subsequently, the CMV promoter was replaced for a CAG promoter.

The ATF6/XBP1s-responsive promoter element of several ATF6/XBP1s binding motifs (2xERSE, 5xUPRE, 4xACGT core), as described in (Du *et al.* 2013), was synthesized and delivered in a pUC19 vector by GenScript (Piscataway, NJ, USA). The ATF6/XBP1s-responsive promoter element controlled transcription of a destabilized green fluorescent protein (GFPd2) amplified from vector pCAG-GFPd2 (gift from Dr. C. Cepko, Department of

Genetics, Harvard University, Boston, MA, USA; RRID:Addgene\_14760; Matsuda and Cepko 2007). A nuclear localization sequence (3  $\times$  PKKKRKV) was fused to the C-terminus of GFPd2 and the complete construct was cloned into pGL4.28[luc2CP/minP/Hygro] (Promega, Madison, WI, USA; E8461).

To generate stable HeLa cell lines, the reporter constructs were transfected using lipofectamine 2000 (Invitrogen; 11668027) into HeLa cells and single colonies were selected using 350  $\mu$ g/mL hygromycin B and tested for their responsiveness to tunicamycin (TM).

#### Pharmaca-based UPR transmission protocol

The pharmaca-based UPR transmission protocol was performed as published before (Mahadevan *et al.* 2011). Cells are either treated with TM (Sigma-Aldrich; T7765) or thapsigargin (TG) (Sigma-Aldrich; T9033) at the concentrations indicated in figure legends to induce the UPR, or treated with vehicle (DMSO, Sigma-Aldrich; D2650 or EtOH). After 2 h incubation, cells were washed two times with culture medium followed by complete medium refreshment before incubation for 24 h (unless otherwise stated in figure legend) to prepare CM. CM was collected and donor cells were lysed with trizol for mRNA analysis or fixed for immunofluorescence. CM was centrifuged (10 min, 268 g) and passed through a sterile 0.2  $\mu$ m filter (VWR; 514-0060) to remove any cellular debris, before the medium of acceptor cells was replaced with CM. After 24 h incubation, acceptor cells were lysed with trizol for mRNA analysis or fixed for immunofluorescence.

#### Co-culture UPR transmission protocol

Mif-inducible IgM heavy chain HeLa cells (Bakunts *et al.* 2017) were co-cultured with (Mif-insensitive) UPR reporter HeLa cells (ATF4 reporter or ATF6/XBP1s reporter) in a 1 : 1 ratio (2500 cells/well each) in a black 96-well plate (Greiner; 655090). Treatment with Mif (0.5 nM; Santa-Cruz; SC-203134) or vehicle (EtOH) was started to induce expression of the IgM heavy chain at 1 day (48 h), 2 days (24 h) and 3 days (6 h) after plating. DMSO/TM/TG treatments were for 24 h. Subsequently, cells were fixed (as described in the Immunofluorescence section), stained with nuclear marker 4',6-diamidino-2-phenylindole (DAPI; 5  $\mu$ g/mL; Invitrogen; D1306) and analyzed using an automated microscopy platform (see Automated microscopy analysis).

#### RNA isolation, cDNA synthesis, and real-time quantitative PCR

Cells were lysed and scraped in TRI Reagent solution (Invitrogen; AM9738). Primary neuron lysates were added to Phase Lock Gel Heavy tubes (Quantabio, Beverly, MA, USA; 733-2478) and organic and aqueous phase separation was initiated by addition of and mixing with chloroform (added in a 1 : 5 ratio; Merck; 1024470500), before centrifugation at 12 000 g for 10 min at 4°C. The RNA-containing aqueous phase was transferred to a fresh tube. RNA isolation was performed using the Isolate II RNA minikit (Bioline, London, UK; BIO-52073) including a DNase treatment and according to the manufacturer's protocols.

For cell lines, chloroform was added to and mixed with the trizol lysates in a 1 : 5 ratio. Organic and aqueous phase separation was achieved by centrifugation at 28 672 g (full speed) for 20 min at 4°C and the aqueous phase was added to a new tube. Chloroform (1 : 5) was added and mixed again to remove more phenol and the mixture was centrifuged at 28 672 g for 5 min at 4°C. The aqueous

phase was separated from the chloroform phase and transferred to a fresh tube. Isopropanol (1:1; VWR Chemicals, Amsterdam, The Netherlands; 1.09634.2500) and glycoblue (1 µL/sample; Invitrogen; AM9516) were added for RNA precipitation and visualizing the pellet. After gently mixing, the mixture was centrifuged at 28 672 *g* for 15 min at 4°C. The supernatant was removed and the pellet was washed with 75% ethanol (Sigma-Aldrich; 16368) and centrifuged at 28 672 *g* for 15 min at 4°C. After removal of ethanol, the pellet was air-dried and dissolved in RNase-free H<sub>2</sub>O.

The NanoDrop 1000 spectrophotometer (Thermo Fisher Scientific, Wilmington, DE, USA) was used to assess RNA concentration, purity and integrity. Synthesis of cDNA was performed using the SensiFAST cDNA Synthesis Kit (Bioline; BIO-65054) according to the manufacturer's protocols.

Per sample 1 µL cDNA was added in triplicate in a 384-well plate suitable for qPCR (Greiner; 785285). Primers and probe (Roche, Indianapolis, IN, USA) combinations are provided in Table 1.

**Table 1** Primers and probes used for qPCR

Target gene	Primer sequence 5'-3'	Universal probe/ SYBR green
mBiP	fw: GCCAACTGTAACAATCAAGGTCT rev: TGACTTCAATCTGGGGAATC	#15
mCHOP	fw: CCACCACCTGAAAGCAG rev: TCCTCATACCAGGCTTCCA	#33
mXBP1s	fw: TCCGCAGCAGGTGCAG rev: CCAACTTGCCAGAATGCC	SYBR green
mEEF1A1	fw: ACACGTAGATTCCGGCAAGT rev: AGGAGCCCTTCCCATCTC	#31
hBiP	fw: GCTGGCCTAAATGTTATGAGGA rev: CCACCCAGGTCAAACACC	#7
hCHOP	fw: AAGGCACTGAGCGTATCATGT rev: TGAAGATACACTTCTTCTTGAACA	#21
hXBP1s	fw: AAGACAGCGCTTGGGGATGG rev: CTGACCTGCTCGGGAC	SYBR green
hXBP1total	fw: GACAGAGAGCCAAAGCTAATGTGG rev: ATCCAGTAGGCAGGAAGAT	SYBR green
hERdj4/ hDNAJB9	fw: CATGAAGTACCACCTGACAAA rev: CATCTGAGAGTGTTCATATGCTTC	#89
hEEF1A1	fw: CAATGGCAAATCTCACTG rev: AACCTCATCTCTATAAAACACCAA	#63
haBiP	fw: CGGCAAGATGAAGTCCCTAT rev: TGCCACATCCTCCTTCTT	#63
haCHOP	fw: TGAGTCCCTGCCTTTTGC rev: CACCTCCTGCAGATCCTCAT	#33
haEEF1A1	fw: AACCGGCCACCTGATCTAC rev: GGCAGCCTCCTTCTCAAAC	#31

BiP, binding immunoglobulin protein; CHOP, C/EBP homologous protein; XBP1s, spliced X-box binding protein 1; EEF1A1, eukaryotic translation elongation factor 1 alpha 1.

Sequence of the primers and their corresponding probes. Probe numbers refer to numbers in the universal probe library (Roche). Mouse (m); human (h); hamster (ha).

**Table 2** PCR cycle parameters

UP/SYBR	Program	Cycles	Temperature, duration, and acquisition mode
UP	Denaturation	1	95°C, 10 min
	Amplification	45	95°C, 10 s; 60°C, 20 s; 72°C, 1 s, single acquisition
	Cooling	1	40°C, 1 s
SYBR	Denaturation	1	95°C, 10 min
	Amplification	40	95°C, 10 s; 60°C, 20 s; 72°C, 1 s, single acquisition
	Melting curve	1	40°C, 1 s; 95°C, continuous acquisition
	Cooling	1	40°C, 1 s

Information on PCR cycle programs for the universal probe (UP) and SYBR green (SYBR) assays.

SensiFAST Probe No-ROX kit (Bioline; BIO-86050) or SensiFAST SYBR No-ROX kit (Bioline; BIO-98050) for XBP1s/unspliced, were added to the primer-probe mixtures to enable the qPCR reaction. PCR cycle parameters are provided in Table 2. The Advanced Relative Quantification analysis of the LightCycler 480 1.5.0 software (Roche; 04994884001) was used for analysis. Data were normalized per experiment and mRNA levels of eukaryotic translation elongation factor 1 alpha 1 are used as reference gene for BiP, C/EBP homologous protein (CHOP), XBP1s, IL-6, and ERdj4. In Fig. 2, presenting data from HeLa and THP-1 cells, XBP1s values are shown as the ratio of XBP1s over XBP1total levels.

#### Immunofluorescence and confocal microscopy

SK-N-SH, HeLa, and co-cultured cells were fixed in 96-well plates with formaldehyde 3.7% (FA; Electron Microscopy Sciences, Hatfield, PA, USA; 15680) in a two-step protocol, first FA was added to the medium (1:1) and incubated for 10 min at 20°C followed by 20 min incubation with 3.7% FA only. Cells were washed and stored in phosphate-buffered saline (PBS; pH 7.4).

For immunofluorescence, cells were permeabilized in 0.5% Triton X-100 (Fisher Chemical, Vantaa, Finland; T/3751/08) in PBS for 5 min and blocked using 0.1% Triton X-100 and 2% goat serum (Gibco; 16210072) for 30 min. Primary and secondary antibodies were diluted in blocking buffer. Primary antibody incubation was performed overnight at 4°C. Primary antibodies and dilutions can be found in Table 3. After three washes in PBS, cells were incubated with Alexa Fluor conjugated secondary antibodies (1:500; Thermo Fisher Scientific, Waltham, MA, USA; A-11008, RRID:AB\_143165, A-21449, RRID:AB\_2535866, A-21235, RRID:AB\_2535804) for 1–2 h at 20°C. Negative stainings (secondary antibody only incubation) were included and used in the automated microscopy analysis as background values. After three washes in PBS (second wash contained the nuclear marker DAPI (5 µg/mL; Invitrogen; D1306) plates were stored in the fridge until further analysis.

SK-N-SH cells overexpressing the active transcription factors ATF6 and XBP1s, were immunostained for BiP (located in the ER) and XBP1 (active XBP1s localizes to the nucleus). MAP2 was used as whole cell marker and DAPI as nuclear marker. Cells were imaged with a NIKON Ti-Eclipse microscope using galvano scanning mode

**Table 3** Primary antibodies

Primary antibody	Dilution	Company, category number and RRID	IF/WB
Rabbit-anti-GRP78 (BiP)	1 : 100	Santa Cruz, sc-13968, RRID:AB_2119991	IF
Rabbit-anti-ATF4	1 : 250	Cell Signaling, #11815, RRID:AB_2616025	IF
Rabbit-anti-XBP1	1 : 1000	Santa Cruz, sc-7160, RRID:AB_794171	IF
Chicken-anti-MAP2	1 : 250	Abcam, ab5392, RRID:AB_2138153	IF
Mouse-anti-Tubulin beta III isoform	1 : 500	Millipore, MAB1637, RRID:AB_2210524	IF
Mouse-anti-GAPDH	1 : 250	Millipore, MAB374, RRID:AB_2107445	IF
Rabbit-anti-Phospho-eIF2 $\alpha$ (Ser51)	1 : 500	Cell Signaling, #9721, RRID:AB_330951	WB
Mouse-anti-Total-eIF2 $\alpha$	1 : 500	Abcam, ab5369, RRID:AB_304838	WB

BiP, binding immunoglobulin protein; ATF4, activating transcription factor 4.

Primary antibodies used for immunofluorescence (IF) or western blotting (WB).

and a 60 $\times$  oil-immersion objective (numerical aperture 1.4). ImageJ software (developed by the National Institutes of Health, Bethesda, MD, USA) was used to select representative images with approximately the same number of cells per field of view.

#### Automated microscopy analysis

Immunofluorescence and direct fluorescence in SK-N-SH and Mif-inducible IgM heavy chain HeLa cells and co-culture UPR reporter assays were imaged using an automated microscopy platform (CellInsight CX7; ThermoFisher Scientific, Waltham, MA, USA). DAPI (nuclear marker) was used for autofocus and immunofluorescence experiments were imaged with a 10 $\times$  objective and 25 fields of view per well and UPR reporter assays with a 20 $\times$  objective and 20 fields of view per well. Image analysis was performed with Columbus 2.5 software (PerkinElmer, Groningen, The Netherlands). For both ATF4 and XBP1 immunostainings as well as UPR reporters, fluorescence intensity in the nucleus (DAPI mask) followed by background subtraction (ring around nucleus) was used as output data. BiP immunofluorescence was measured in a whole cell mask [either MAP2, Tubulin beta III isoform (SK-N-SH cells) or GAPDH (IgM heavy chain HeLa cells)]. Negative stainings (secondary antibody only incubation) were also used to determine background values for immunofluorescence experiments and values were subtracted from output data of ATF4, XBP1, and BiP analyses. In experiments with SK-N-SH cells, the highest and lowest data points (one pair/experiment) were excluded from the datasets. Data of UPR reporter experiments were normalized by rescaling between 1 (minimum; EtOH/Mif 48 h) and 10 (maximum; TG) per experiment.

#### Sodium dodecyl sulfate–polyacrylamide gel electrophoresis and western blotting

Cells were lysed in freshly prepared ice-cold PBS with 1% Triton X-100 (Fisher Chemical; T/3751/08), protease inhibitors (Roche; 4693116001) and phosphatase inhibitor cocktails (Roche; 4906845001). Cells were incubated for 15 min on ice before they were scraped, collected and cleared by centrifugation for 20 min at 10 000 *g* and 4°C. Total protein concentration in the supernatants was determined by a Bradford protein assay (Bio-Rad Laboratories, Hercules, CA, USA; 500-00006). Equal amounts of protein (23  $\mu$ g) were separated on a 10% sodium dodecyl sulfate/polyacrylamide gel. Proteins were transferred to nitrocellulose membranes (Bio-Rad; 1620115) using a semi-dry electro blotting apparatus. Membranes

were briefly washed in Tris-buffered saline with Tween 20 (TBS-T) (Sigma-Aldrich; P9416) before 1 h incubation in blocking buffer (5% bovine serum albumin (Acros Organics, Geel, Belgium; ACRO268131000) in TBS-T). Primary antibodies (see Table 3) were diluted in blocking buffer and membranes were incubated overnight at 4°C. After washing in TBS-T, membranes were incubated with horseradish peroxidase-labeled antibodies (1 : 2000; Dako, Carpinteria, CA, USA; P0448, RRID:AB\_2617138 and P0447, RRID:AB\_2617137) in blocking buffer for 1 h at 20°C and again washed in TBS-T. Reactive protein bands were developed using the Lumi-Light reagent (Roche; 12015196001) for 5 min and visualized on the Odyssey Imaging System (LI-COR, Lincoln, NE, USA). Intensity of protein bands was quantified with Image Studio 2.0 software (LI-COR), using the ratio of phospho-eIF2 $\alpha$  over total eIF2 $\alpha$  signal.

#### Study design and statistical analysis

The study was exploratory and not pre-registered. No randomization was performed for the animals, because the mice were only used for isolation of primary neurons. No statistical method was used to determine sample size or outliers and no data were excluded unless specifically stated. Researchers were not blinded to the experimental conditions.

Graphpad Prism 8.1.1 software (GraphPad Software Inc., San Diego, CA, USA) was used to perform statistical analysis. To determine if data were normally distributed the Shapiro–Wilk test was used. The statistical tests used to determine significant differences between experimental groups are indicated in each figure legend. One-way ANOVA was used to test significant differences between three or more experimental groups, followed by Sidak's multiple comparisons test. The Kruskal–Wallis test followed by Dunn's multiple comparisons test was used as nonparametric alternative. The one-sample or unpaired *t*-test (two-tailed) was performed to determine whether the experimental group was statistically different compared to the vehicle group. Bar graph values represent mean  $\pm$  SEM and graphs also show individual data points representing the number of independent cell culture preparations (*N*) for qPCR experiments or all the biological replicates from multiple cell culture preparations as is mentioned in figure legends. In case of *N* = 1, error bars represent the variation (SEM) between *n* = 3 technical replicates, in case of *N*  $\geq$  2, error bars represent the variation (SEM) between the means of the experiments. A *p* value < 0.05 was considered statistically significant. \**p* < 0.05, \*\**p* < 0.01, \*\*\**p* < 0.001, ns indicates not significant.

### Availability of data and materials

Data and custom-made materials from this study are available from the corresponding author upon reasonable request.

## Results

### Pharmaca-based UPR transmission in neuronal cells

Because of the relevance of UPR signaling in the pathogenesis of neurodegenerative diseases, we studied cell-to-cell UPR transmission in neuronal cells. To this end, we employed a pharmaca-based UPR transmission protocol (originally published by Mahadevan *et al.* 2011) in murine primary neurons and human differentiated neuronal SK-N-SH cells. In this protocol, the UPR is activated by treatment with TM, an inhibitor of N-linked glycosylation (Tkacz and Lampen 1975; Takatsuki, Kohno, and Tamura 1975) or TG (a non-competitive inhibitor of the sarcoplasmic/ER  $\text{Ca}^{2+}$  ATPase pump; Lyttonsg, Westlins, and Hanleyll 1991). After 2 h of TM/TG treatment, the cells were washed twice to remove the chemical stressor followed by a complete medium change to generate CM from these 'donor' cells, either prepared using TM as UPR inducer (TM-CM) or TG (TG-CM). Subsequently CM was transferred to naive ('acceptor') cells in a fresh culture dish and incubated for another 24 h. UPR activation was analyzed in both donor and acceptor cells by qPCR and automated immunofluorescence microscopy to determine the mRNA and protein levels, respectively, of targets representing all three UPR pathways; BiP (ATF6 target), CHOP and ATF4 (PERK targets) and the spliced variant of XBP1 (XBP1s; IRE1 target; Lee, Iwakoshi, and Glimcher 2003; Lu *et al.* 2004; Adamson *et al.* 2016).

Using the pharmaca-based UPR transmission protocol, TM-CM was prepared in either 1, 4, or 24 h before transfer to naive acceptor cells (Fig. S1a and d). We observed increased mRNA and protein expression of UPR targets in neuronal donor (Fig. S1b,e and S2b) as well as acceptor cells (Fig. S1c,f and S2c), reproducing the published results obtained using tumor cells and macrophages (Mahadevan *et al.* 2011) and neuronal cells (Sprenkle *et al.*, 2019). However, whereas UPR activation increased over time in donor cells, the CM-induced UPR activation in acceptor cells at 1 h reached maximum levels and did not show this increase at subsequent time points (Fig. S1). This indicates that there is no direct correlation between the extent of UPR activation in the donor cells and that in the acceptor cells.

### Carry-over of TM and TG is a confounding factor in pharmaca-based UPR transmission protocols

Despite the washing procedure, the use of pharmacological compounds to generate the CM bears a potential artefact by carry-over of the pharmaca. To establish that UPR activation in acceptor cells is due to transmission of a signal secreted by the donor cells rather than by residual pharmaca, we

performed mass spectroscopy to check the levels of pharmaca in the CM, as was previously used as carry-over control experiment (Mahadevan *et al.* 2011). However, injecting TG in aqueous solution (like CM) leads to retention of the stressor in the mass spectroscopy system, probably due to its poor solubility. Indeed, residual TG was detected upon subsequent washing of the mass spectroscopy system (data not shown). This hampered reliable measurement of TG in the CM, therefore an alternative carry-over control experiment was essential.

To this end, the same UPR transmission protocol was performed in the presence or absence of donor cells (Fig. 1a and Fig. S2a). Upon incubation of naive SK-N-SH acceptor cells with TM-CM (Fig. 1b and Fig. S2c) or TG-CM (Fig. 1c and Fig. S2c) prepared in the presence and in the absence of donor cells, BiP, CHOP, and XBP1s mRNA levels (Fig. 1b and c) and BiP, ATF4, and XBP1s protein levels (Fig. S2c) were increased compared to incubation with vehicle-CM. Although in some cases a slightly stronger response was observed by CM generated in the presence of donor cells, TM-CM and to a stronger extent TG-CM generated in the absence of donor cells robustly induced the mRNA and protein levels of UPR targets in acceptor cells (Fig. 1b and c and Fig. S2c).

In addition, generating the CM in coated culture dishes (as used in experiments with primary neurons as donors) without cells, showed a full UPR response in acceptor neurons with two TM-CM concentrations and TG-CM: mRNA levels of BiP, CHOP, and XBP1s were increased compared to vehicle-CM (Fig. 1d).

These experiments demonstrate that carry-over of TM and TG is a major confounding factor in pharmaca-based UPR transmission protocols.

### Genetic induction of single pathways of the UPR does not result in UPR transmission

To further investigate whether cell-to-cell UPR transmission is only an artifact of the pharmaca-based protocol or a real phenomenon, we developed transmission protocols that do not rely on pharmaca. First, we employed genetic tools inducing single pathways of the UPR. Chinese hamster ovary (CHO) cells stably expressing the kinase domain of PERK coupled to 2 Fv receptor domains (Fv2E-PERK; Lu *et al.* 2004) were used to specifically activate downstream PERK signaling upon addition of the homodimerizer (Spencer *et al.* 1993) and to prepare CM (Fig. S3). To selectively activate the ATF6 and IRE1 pathways of the UPR, SK-N-SH cells overexpressing the doxycycline-inducible active transcription factors ATF6 or XBP1s, respectively, were employed to prepare CM (Fig. S4).

Activation of downstream targets by Fv2E-PERK as previously reported (Lu *et al.* 2004), was confirmed by a dose-dependent increase in CHOP mRNA (Fig. S3c) and phosphorylation of eukaryotic initiation factor  $2\alpha$  (P-eIF2 $\alpha$ ;

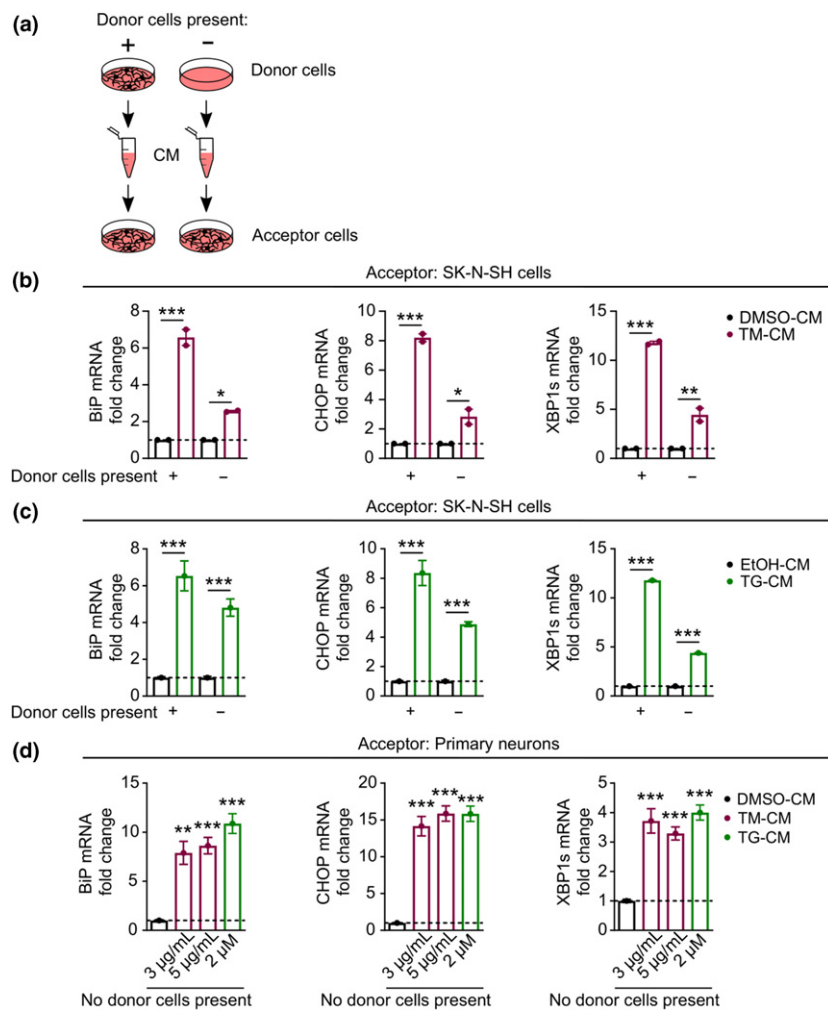


**Fig. 1** Carry-over of tunicamycin (TM) and thapsigargin (TG) in a pharmacobased unfolded protein response (UPR) transmission protocol. (a) Schematic representation of a pharmacobased UPR transmission experiment (Mahadevan *et al.* 2011) performed in parallel with a carry-over control experiment following the exact same protocol in the absence of donor cells. (b, c) SK-N-SH cells were treated for 24 h with DMSO-conditioned media (CM) (vehicle; b), EtOH-CM (vehicle; c), TM-CM (10 µg/mL; b) or TG-CM (5 µM; c) prepared in 1–4 h from SK-N-SH cells or prepared from a parallel experiment without donor cells.  $N = 2$  (b) and  $N = 1$  (c) independent cell culture preparations (shown as individual data points), with  $n = 3$  technical replicates/experiment. (d)

Primary mouse neurons were treated for 24 h with DMSO-CM (vehicle), TM-CM (3 or 5 µg/mL), or TG-CM (2 µM) prepared from an experiment without donor cells.  $N = 1$  independent cell culture preparation (shown as individual data points), with  $n = 3$  technical replicates. Expression levels of UPR target genes binding immunoglobulin protein (BiP), C/EBP homologous protein (CHOP), and X-box binding protein 1 (XBP1s) were analyzed by qPCR (b–d). Data are represented as fold change over respective control conditions (DMSO-CM +/- donor cells present). Significant differences were measured by one-way ANOVA followed by Sidak's multiple comparisons test, conditions were compared to respective control (b–d).

direct substrate of the PERK kinase; Fig. S3d) in response to homodimerizer.

The overexpression and activity of the active transcription factors ATF6 and XBP1s was confirmed by immunostainings of UPR proteins BiP and nuclear XBP1 (Fig. S4a) and the downstream upregulation of the respective UPR targets in donor cells by analysis of the mRNA levels of BiP, CHOP, and ERdj4 (Fig. S4c; the latter is a downstream target of both

ATF6 and XBP1s; Lee, Iwakoshi, and Glimcher 2003; Adamson *et al.* 2016).

However, in contrast to TM-CM, no UPR response was elicited in acceptor SK-N-SH cells treated with CM from any of the donor cells where the UPR pathways were selectively activated (Figs. S3e, f and S4d). This indicates that activation of a single pathway of the UPR is not sufficient to induce UPR transmission.

### Non-pharmacological full UPR activation does not result in UPR transmission

Because it is conceivable that UPR transmission requires full UPR activation, pharmaca-free paradigms activating all three branches of the UPR were tested. Nutrient deprivation for either 6 or 20 h was used to activate the UPR in donor SK-N-SH cells, before CM (supplemented with nutrients) was incubated with acceptor SK-N-SH cells (Fig. S5a). The full UPR was induced upon nutrient deprivation in donor cells as demonstrated by increased BiP, CHOP, and XBP1s mRNA expression (Fig. S5b and c). In contrast, incubation of acceptor cells with CM prepared by nutrient deprivation for 6 or 20 h did not affect the expression of UPR target genes (Fig. S5d and e).

In addition, a genetic model where all three UPR pathways are activated was employed. A stable HeLa cell line harboring mifepristone (Mif)-inducible expression of immunoglobulin M (IgM) heavy chain was used to induce all three branches of the UPR (Bakunts *et al.* 2017) in donor cells (Fig. 2a and Fig. S6a). As previously shown (Bakunts *et al.* 2017), 24 h incubation with Mif induced UPR targets as demonstrated by significantly increased mRNA levels of BiP and XBP1s as well as a strong trend for CHOP (Fig. 2b) and significantly increased protein levels of BiP, ATF4, and XBP1s (Fig. S6a). Mif-insensitive human monocytic THP-1 cells differentiated towards a macrophage-like phenotype were employed as acceptor cells (Fig. 2a). THP-1 cells showed increased mRNA levels of BiP, CHOP, and XBP1s upon treatment for 24 h with TM-CM, but not with Mif-CM (Fig. 2c). TLR4, has been suggested to mediate UPR transmission from tumor cells to macrophage acceptor cells (Mahadevan *et al.* 2011). The differentiated THP-1 macrophages we used here express TLR4 as demonstrated by the strong increase in mRNA expression of the pro-inflammatory cytokine interleukin-6 (IL-6; 64.4-fold) upon treatment with the TLR4 agonist LPS (Fig. 2d). This excludes the absence of this receptor as explanation for the incapability of the Mif-CM to induce the UPR in acceptor cells. We therefore conclude that non-pharmacological activation of a full UPR by nutrient deprivation or a genetic tool does not lead to UPR transmission.

### Genetically-induced full UPR activation does not result in UPR transmission in co-culture

The transmission experiments presented above are based on the transfer of CM from donor to acceptor cells. To ascertain a continuous exposure to potential transmission factors, the Mif-inducible IgM heavy chain HeLa donor cells were co-cultured together with either ATF4 or ATF6/XBP1s reporter HeLa acceptor cells. Both reporter lines express a nuclear fluorescent signal upon UPR activation (Fig. 2e). The co-cultures were treated with either vehicle or increasing concentrations of TM or TG for 24 h. Nuclear

fluorescence of both reporters was analyzed using automated microscopy (Fig. 2e). TM induced a significant and dose-dependent increase in the reporter cell lines. In addition, TG also significantly induced the reporter signal. These results validate the UPR reporter cell lines and demonstrate their sensitivity. In contrast, Mif treatment for 6, 24, or 48 h did not induce the fluorescent signal in either of the acceptor reporter cell lines (Fig. 2f; representative images of a co-culture experiment using both UPR reporters are shown in Fig. S6b–d). Therefore, also in co-culture genetic induction of a full UPR did not result in UPR transmission.

## Discussion

The data we present here demonstrate that pharmaca-based cell culture protocols are unsuitable to study UPR transmission because carry-over of the pharmaca is a strong confounding factor. In addition, we find no evidence for *in vitro* UPR transmission using different non-pharmacological UPR induction paradigms, both by nutrient deprivation and by genetic tools. Also in direct co-culture, no UPR transmission is observed using non-pharmacological UPR induction. This indicates not only that the interpretation of studies using pharmacological induction of the UPR to study transmission is hampered by methodological artifacts, but also brings up the question whether UPR transmission is a real phenomenon.

*In vivo* studies have reported that genetic activation of single UPR signaling pathways in one tissue results in UPR activation in another. In *C. elegans*, neuron-specific expression of constitutively active XBP1s induces UPR activation in the intestine. Interestingly, the cell non-autonomous signals extend the lifespan of the animals and makes them more resistant to ER stress (Taylor and Dillin 2013). In mice, selective XBP1s expression in pro-opiomelanocortin neurons results in activation of an XBP1s-mediated transcriptional response in the liver and improves glucose homeostasis (Williams *et al.* 2014). This may suggest that in the context of physiological anatomical contacts, cell-to-cell exchange of UPR signaling may occur from neurons to peripheral organs. Possibly, the sensitivity or response to UPR-induced neuronal signals may differ between organs. Alternatively, the overexpression of XBP1s in the 'donor organ' results in the secretion of one or multiple factor(s) that elicit activation of the IRE1 pathways of the UPR, resulting in increased XBP1s levels. Indeed, unconventional protein secretion is induced by UPR activation (Gee *et al.* 2011; Jung *et al.* 2016; Bel *et al.* 2017; van Ziel *et al.* 2019) and has been hypothesized to mediate stress-induced danger signaling (Dupont *et al.* 2011; Zhu *et al.* 2011).

Our data instigate further critical investigation of the cell non-autonomous UPR where the focus should shift from



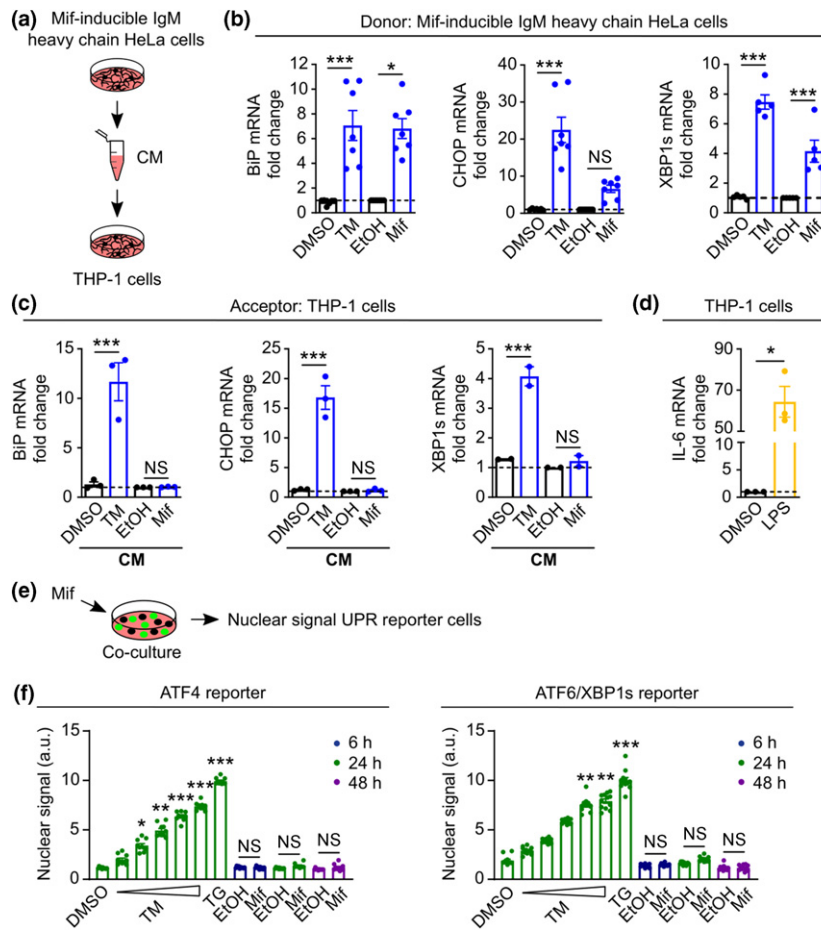


**Fig. 2** Genetic induction of a full unfolded protein response (UPR) does not result in UPR transmission. (a) Schematic representation of a UPR transmission experiment performed with mifepristone (Mif)-inducible immunoglobulin M (IgM) heavy chain HeLa cells (Bakunts *et al.* 2017) as donors of conditioned media (CM) and THP-1 cells as Mif-insensitive acceptor cells. (b) Mif-inducible IgM heavy chain HeLa cells treated for either 2 h with DMSO (vehicle) and TM (3  $\mu$ g/mL) followed by two washes and subsequent replacement of total medium and 24 h incubation to prepare CM, or treated with EtOH (vehicle) and Mif (0.5 nM) for 24 h to prepare CM. After CM collection, mRNA expression levels were analyzed by qPCR of UPR target genes binding immunoglobulin protein (BiP), C/EBP homologous protein (CHOP) and X-box binding protein 1 (XBP1s). Data are presented as fold change difference over control (EtOH, set to 1).  $N = 7$  (BiP/CHOP) and  $N = 5$  (XBP1s) independent cell culture preparations (shown as individual data points), with  $n = 3$  technical replicates/experiment. (c) THP-1 cells were treated for 24 h with DMSO-CM, TM-CM, EtOH-CM or Mif-CM prepared as in (b). qPCR analysis of UPR target genes BiP, CHOP and XBP1s was performed. Data are presented as fold change difference over control (EtOH, set to 1).  $N = 3$  (BiP/CHOP) and  $N = 2$  (XBP1s) independent cell culture preparations (shown as individual data points), with  $n = 3$  technical replicates/experiment. Significant differences were measured by one-way ANOVA followed by Sidak's multiple comparisons test (b, c), all conditions were compared to respective

control (DMSO/EtOH). (d) THP-1 cells were treated with DMSO (vehicle) or LPS (100 ng/mL) for 24 h. Expression levels of IL-6 mRNA were determined by qPCR analysis. Data are presented as fold change difference over control (DMSO, set to 1). Significant differences were measured by one-sample *t*-test (two-tailed) compared to DMSO.  $N = 3$  independent cell culture preparations (shown as individual data points), with three technical replicates/experiment. (e) Schematic representation of the experimental set-up for UPR transmission in co-culture of Mif-inducible IgM heavy chain HeLa cells (Bakunts *et al.* 2017) and Mif-insensitive UPR reporter HeLa cells (activating transcription factor 4, ATF4 reporter or activating transcription factor 6 (ATF6)/XBP1s reporter). Upon UPR activation, the UPR reporter cells express a nuclear fluorescent signal. (f) Co-cultured cells [as described in (e)] were treated with DMSO (vehicle), increasing concentrations of TM (0.0625–1  $\mu$ g/mL) and thapsigargin (TG) (0.5  $\mu$ M) for 24 h, or treated with EtOH (vehicle) or Mif (0.5 nM) for 6, 24, or 48 h. Cells were fixed and stained with DAPI (nuclear marker) before image analysis of nuclear fluorescent signal using automated microscopy. Representative images of co-culture experiments are presented in Fig. S6b–d.  $N = 3$  independent cell culture preparations with  $n = 4$  biological replicates/experiment [shown as individual data points in arbitrary units (a.u.)]. Significant differences were measured by the Kruskal–Wallis test followed by Dunn's multiple comparisons test (f), all conditions were compared to respective control (DMSO/EtOH).

transmission of UPR activity to factors that are secreted upon UPR activation and their downstream effects.

## Conclusion

In conclusion, carry-over of pharmaca is a major confounding factor in pharmaca-based UPR transmission protocols that are therefore unsuitable to study cell-to-cell UPR transmission. In addition, the absence of UPR transmission in non-pharmaca-based models of UPR activation indicates that cell-to-cell UPR transmission does not occur in cell culture.

## Acknowledgments and conflict of interest disclosure

We thank Ingrid Saarloos and Robbert Zalm for cloning and producing viral particles, Desiree Schut for primary neuron culture, Jurjen Broeke for expert help with confocal microscopy and Rob Zwart and Fabian Bangel for general laboratory support. We thank David Ron for providing the Fv2E-PERK-expressing CHO cell line and for scientific discussion and Jeroen Hoozemans for the THP-1 cells. We thank Matthijs Verhage for scientific discussion and the Molecular Neurodegeneration group (Functional Genomics, VU university, Amsterdam) for critical reading of the manuscript and discussion. This study was supported by grants from Deltaplan Dementie (ZonMW Memorabel/Alzheimer Nederland 733050101) and Weston Brain Institute (NR160014) to WS. The authors declare no conflict of interest.

All experiments were conducted in compliance with the ARRIVE guidelines.

## Open science badges

This article has received a badge for \*Open Materials\* because it provided all relevant information to reproduce the study in the manuscript. The complete Open Science Disclosure form for this article can be found at the end of the article. More information about the Open Practices badges can be found at <https://cos.io/our-service/open-science-badges/>

## Supporting information

Additional supporting information may be found online in the Supporting Information section at the end of the article.

**Figure S1.** UPR activation in donor and acceptor neuronal cells in a pharmaca-based UPR transmission protocol.

**Figure S2.** Carry-over of TM and TG in a pharmaca-based UPR transmission protocol.

**Figure S3.** Genetic induction of the PERK pathway of the UPR does not result in UPR transmission.

**Figure S4.** Genetic induction of the ATF6 or IRE1 pathway of the UPR does not result in UPR transmission.

**Figure S5.** Physiological UPR activation by nutrient deprivation does not result in UPR transmission.

**Figure S6.** Genetic induction of a full UPR does not result in UPR transmission in co-culture.

## References

- Adamson B., Norman T. M., Jost M., *et al.* (2016) A multiplexed single-cell CRISPR screening platform enables systematic dissection of the unfolded protein response. *Cell* **167**, 1867–1882.e21.
- Bakunts A., Orsi A., Vitale M., Cattaneo A., Lari F., Tadè L., Sitia R., Raimondi A., Bachi A. and Van Anken E. (2017) Ratiometric sensing of BiP-client versus BiP levels by the unfolded protein response determines its signaling amplitude. *ELife* **6**, e27518.
- Bel S., Pendse M., Wang Y., *et al.* (2017) Paneth cells secrete lysozyme via secretory autophagy during bacterial infection of the intestine. *Science* **357**, 1047–1052.
- Du Z., Treiber D., McCoy R. E., Miller A. K., Han M., He F., Domnitz S., Heath C. and Reddy P. (2013) Non-invasive UPR monitoring system and its applications in CHO production cultures. *Biotechnol. Bioeng.* **110**, 2184–2194.
- Dupont N., Jiang S., Pilli M., Ornatowski W., Bhattacharya D. and Deretic V. (2011) Autophagy-based unconventional secretory pathway for extracellular delivery of IL-1 $\beta$ . *EMBO J.* **30**, 4701–4711.
- Gee H. Y., Noh S. H., Tang B. L., Kim K. H. and Lee M. G. (2011) Rescue of  $\Delta$ F508-CFTR trafficking via a GRASP-dependent unconventional secretion pathway. *Cell* **146**, 746–760.
- Gerakis Y. and Hetz C. (2018) Emerging roles of ER stress in the etiology and pathogenesis of Alzheimer's disease. *FEBS J.* **285**, 995–1011.
- Goedert M. (2015) Neurodegeneration. Alzheimer's and Parkinson's diseases: the prion concept in relation to assembled A $\beta$ , tau, and  $\alpha$ -synuclein. *Science* **349**, 6248, 1255555.
- Halliday M., Hughes D. and Mallucci G. R. (2017) Fine-tuning PERK signaling for neuroprotection. *J. Neurochem.* **142**, 812–826.
- Jung J., Kim J., Roh S. H., Jun I., Sampson R. D., Gee H. Y., Choi J. Y. and Lee M. G. (2016) The HSP70 co-chaperone DNAJC14 targets misfolded pendrin for unconventional protein secretion. *Nat. Commun.* **7**, 1–15.
- Lee A., Iwakoshi N. N. and Glimcher L. H. (2003) XBP-1 regulates a subset of endoplasmic reticulum resident chaperone genes in the unfolded protein response. *Mol. Cell. Biol.* **23**, 7448–7459.
- Lee Y., Cevallos R. C. and Jan E. (2009) An upstream open reading frame regulates translation of GADD34 during cellular stresses that induce EIF2 $\alpha$  phosphorylation. *J. Biol. Chem.* **284**, 6661–6673.
- Lu P. D., Jousse C., Marciniak S. J., Zhang Y., Novoa I., Scheuner D., Kaufman R. J., Ron D. and Harding H. P. (2004) Cytoprotection by pre-emptive conditional phosphorylation of translation initiation factor 2. *EMBO J.* **23**, 169–179.
- Lyttonsg J., Westlins M. and Hanleyll M. R. (1991) Thapsigargin inhibits the sarcoplasmic or endoplasmic reticulum Ca-ATPase family of calcium pumps. *J. Biol. Chem.* **266**, 17067–17071.
- Mahadevan N. R., Rodvold J., Sepulveda H., Rossi S., Drew A. F. and Zanetti M. (2011) Transmission of endoplasmic reticulum stress and pro-inflammation from tumor cells to myeloid cells. *Proc. Natl Acad. Sci. USA* **108**, 6561–6566.
- Matsuda T. and Cepko C. L. (2007) Controlled expression of transgenes introduced by in vivo electroporation. *Proc. Natl Acad. Sci. USA* **104**, 1027–1032.
- Matzinger P. (1994) Tolerance, danger, and the extended family. *Annu. Rev. Immunol.* **12**, 991–1045.
- van Oosten-Hawle P. and Morimoto R. I. (2014) Organismal proteostasis: role of cell-nonautonomous regulation and transcellular chaperone signaling. *Genes Dev.* **28**, 1533–1543.
- Rodvold J. J., Chiu K. T., Hiramatsu N., Nussbacher J. K., Galimberti V., Mahadevan N. R., Willert K., Lin J. H. and Zanetti M. (2017) Intercellular transmission of the unfolded protein response

- promotes survival and drug resistance in cancer cells. *Sci. Signal.* **10**, 482.
- Scheper W. and Hoozemans J. J. M. (2015) The unfolded protein response in neurodegenerative diseases: a neuropathological perspective. *Acta Neuropathol.* **130**, 315–331.
- Schinzel R. and Dillin A. (2015) Endocrine aspects of organelle stress – cell non-autonomous signaling of mitochondria and the ER. *Curr. Opin. Cell Biol.* **33**, 102–110.
- Spencer D. M., Wandless T. J., Schreiber S. L. and Crabtree G. R. (1993) Controlling signal transduction with synthetic ligands. *Science* **262**, 1019–1024.
- Sprenkle N. T., Lahiri A., Simpkins J. W. and Meares G. P. (2019) Endoplasmic reticulum stress is transmissible in vitro between cells of the central nervous system. *J. Neurochem.* **148**, 516–530.
- Takatsuki A., Kohno K. and Tamura G. (1975) Inhibition of biosynthesis of polyisoprenol sugars in chick embryo microsomes by tunicamycin. *Agric. Biol. Chem.* **39**, 2089–2091.
- Taylor R. C. and Dillin A. (2013) XBP-1 is a cell-nonautonomous regulator of stress resistance and longevity. *Cell* **153**, 1435–1447.
- Tkacz J. S. and Lampen J. O. (1975) Tunicamycin inhibition of polyisoprenyl *N*-acetylglucosaminyl pyrophosphate formation in calf-liver microsomes. *Biochem. Biophys. Res. Commun.* **65**, 248–257.
- Van Ziel A. M., Largo-Barrientos P., Wolzak K., Verhage M. and Scheper W. (2019) Unconventional secretion factor GRASP55 is increased by pharmacological unfolded protein response inducers in neurons. *Sci. Rep.* **9**, 1567.
- Walter P. and Ron D. (2011) The unfolded protein response: from stress pathway to homeostatic regulation. *Science* **334**, 1081–1086.
- Williams K. W., Liu T., Kong X., *et al.* (2014) Xbp1s in Pomc neurons connects ER stress with energy balance and glucose homeostasis. *Cell Metab.* **20**, 471–482.
- Zanetti M., Rodvold J. J. and Mahadevan N. R. (2016) The evolving paradigm of cell-nonautonomous UPR-based regulation of immunity by cancer cells. *Oncogene* **35**, 269–278.
- Zhu H., Wang L., Ruan Y., *et al.* (2011) An efficient delivery of DAMPs on the cell surface by the unconventional secretion pathway. *Biochem. Biophys. Res. Commun.* **404**, 790–795.

## Open Practices Disclosure

**Manuscript Title:** No evidence for cell-to-cell transmission of the unfolded protein response in cell culture

**Corresponding Author:** Wiep Scheper

Articles accepted to *Journal of Neurochemistry* after 01.2018 are eligible to earn badges that recognize open scientific practices: publicly available data, material, or preregistered research plans. Please read more about the badges in our *author guidelines and Open Science Badges page*, and you can also find information on the Open Science Framework [wiki](#).

Please check this box if you are interested in participating.

To apply for one or more badges acknowledging open practices, please check the box(es) corresponding to the desired badge(s) below and provide the information requested in the relevant sections. To qualify for a badge, you must provide a URL, doi, or other permanent path for accessing the specified information in a public, open-access repository. **Qualifying public, open-access repositories are committed to preserving data, materials, and/or registered analysis plans and keeping them publicly accessible via the web in perpetuity.** Examples include the Open Science Framework ([OSF](#)) and the various Dataverse networks. Hundreds of other qualifying data/materials repositories are listed at <http://re3data.org/>. Preregistration of an analysis plan must take place via a publicly accessible registry system (e.g., [OSF](#), [ClinicalTrials.gov](#) or other trial registries in the [WHO Registry Network](#), institutional registration systems). **Personal websites and most departmental websites do not qualify as repositories.**

Authors who wish to publicly post third-party material in their data, materials, or preregistration plan must have the proper authority or permission agreement in order to do so.

There are circumstances in which it is not possible or advisable to share any or all data, materials, or a research plan publicly. For example, there are cases in which sharing participants' data could violate confidentiality. If you would like your article to include an explanation of such circumstances and/or provide links to any data or materials you have made available—even if not under conditions eligible to earn a badge—you may write an alternative note that will be published in a note in the article. Please check this box if you would like your article to include an alternative note and provide the text of the note below:

**Alternative note:**

## Open Data Badge

1. Provide the URL, doi, or other **permanent path** for accessing the data in a **public, open-access repository**:

Confirm that there is sufficient information for an independent researcher to reproduce **all of the reported results**, including codebook if relevant.

Confirm that you have registered the uploaded files so that they are **time stamped** and cannot be age.

## Open Materials Badge

1. Provide the URL, doi, or other **permanent path** for accessing the materials in a **public, open-access repository**: all relevant information is provided in the manuscript and custom-made materials will be provided upon reasonable request.

Confirm that there is sufficient information for an independent researcher to reproduce **all of the reported methodology**.

Confirm that you have registered the uploaded files so that they are **time stamped** and cannot be age.

## Preregistered Badge

1. Provide the URL, doi, or other **permanent path** to the registration in a **public, open-access repository**\*

2. Was the analysis plan registered prior to examination of the data or observing the outcomes? If no, explain.\*\*

3. Were there additional registrations for the study other than the one reported? If yes, provide links and explain.\*

\*No badge will be awarded if (1) is not provided, or if (3) is answered "yes" without strong justification

\*\*If the answer to (2) is "no," the notation DE (Data Exist) will be added to the badge, indicating that registration postdates realization of the outcomes but predates analysis.

By printed date and name (handwritten) below, authors affirm that the above information is accurate and complete, that any third-party material has been reproduced or otherwise made available only with the permission of the original author or copyright holder, and that publicly posted data do not contain information that would allow individuals to be identified without consent.

***Please do not add your signature to avoid any misuse, as this form will be published with the manuscript.***

Date:

19-08-2019

Handwritten Name (\*not\* signature):

